Inclusive Electron Scattering And The GENIE Neutrino Event Generator

A. Papadopolou,[1] A. Ashkenazi,[1, *] S. Gardiner,[2] M. Betancourt,[2] S. Dytman,[3] L.B. Weinstein,[4]
E. Piasetzky,[5] F. Hauenstein,[4, 1] M. Khachatryan,[4] S. Dolan,[6] G. Megias,[7] and O. Hen[1]

[1]*Massachusetts Institute of Technology, Cambridge, Massachusetts 02139, USA*
[2]*Fermi National Accelerator Laboratory, Batavia, IL*
[3]*University of Pittsburgh, Pittsburgh, PA*
[4]*Old Dominion University, Norfolk, Virginia 23529*
[5]*School of Physics and Astronomy, Tel Aviv University, Tel Aviv 69978, Israel*
[6]*CERN, European Organization for Nuclear Research, Geneva, Switzerland*
[7]*Research Center for Cosmic Neutrinos, Institute for Cosmic Ray
Research, University of Tokyo, Kashiwa, Chiba 277-8582, Japan*
(Dated: September 16, 2020)

————————

The $e4\nu$ collaboration

The extraction of neutrino mixing parameters from accelerator-based neutrino oscillation experiments relies on proper modeling of neutrino-nucleus scattering processes using neutrino interaction event generators. Experimental tests of these generators are made more difficult by the broad range of neutrino energies produced in accelerator-based beams and the low statistics of current experiments. Here we overcome this difficulty by exploiting the similarity of neutrino and electron interactions with nuclei to test neutrino event generators using high-precision inclusive electron scattering data. To this end we revised the electron-scattering mode of the GENIE event generator (e-GENIE) to include electron-nucleus bremsstrahlung radiation effects and to use the exact same physics models and, when relevant, model parameters, as the standard neutrino-scattering version. We also implemented new models for quasielastic (QE) scattering and meson exchange currents (MEC) based on the theory-inspired SuSAv2 approach. Comparing the new e-GENIE predictions with inclusive electron scattering data, we find an overall adequate description of the data in the QE- and MEC-dominated lower energy transfer regime, especially when using the SuSAv2 models. Higher energy transfer-interactions, which are dominated by resonance production, are still not well modeled by e-GENIE.

Introduction

The extraction of neutrino mixing parameters from neutrino oscillation experiments relies on comparing the energy-dependent neutrino flux $\Phi_i(E, L)$ for neutrino flavor ν_i near the neutrino production point ($L \approx 0$) with that at a significant distance L away. In practice, the flux is extracted from the measured neutrino-nucleus interactions in a detector, $N_i(E_{\rm rec}, L)$, where $E_{\rm rec}$ is the incident neutrino energy, as reconstructed from the measured particles ejected in the neutrino-nucleus interaction. Extracting $\Phi_i(E, L)$ from $N_i(E_{\rm rec}, L)$ therefore requires knowledge of the ν-nucleus interaction processes.

The measured interaction rate is related to the incident neutrino flux via

$$N(E_{\rm rec}, L) \propto \sum_i \int \Phi(E, L)\sigma_i(E)f_{\sigma_i}(E, E_{\rm rec})dE, \quad (1)$$

where $\sigma_i(E)$ is the neutrino interaction cross-section for process i and $f_{\sigma_i}(E, E_{\rm rec})$ is a neutrino energy smearing matrix that relates the real and experimentally-reconstructed neutrino energies. The precision with which one can model $\sigma_i(E)$ and $f_{\sigma_i}(E, E_{\rm rec})$ determines the precision with which one can extract the neutrino

flux. This in turn fixes the precision of the extracted oscillation parameters.

Our knowledge of $\sigma_i(E)$ and $f_{\sigma_i}(E, E_{\rm rec})$ is encapsulated in *event generators*, computer programs which implement neutrino interaction models suitable for use in Monte Carlo simulations. Due to the critical role played by neutrino event generators in the analysis and interpretation of data obtained by oscillation experiments, testing and improving generator physics models is essential for reducing systematic uncertainties in precision neutrino experiments. However, due to the broadband nature of accelerator-based neutrino beams (i.e., their wide range of neutrino energies) and the limited statistics available from current experiments, it is very difficult to measure differential neutrino-nucleus cross sections for specific neutrino energies and to test beam energy reconstruction techniques.

Because neutrinos and electrons are both leptons, they interact with atomic nuclei in similar ways (see Fig. 1). Electrons interact via a vector current ($j^\mu_{EM} = \bar{u}\gamma^\mu u$) and neutrinos interact via vector and axial-vector ($j^\mu_{CC} = \bar{u}\gamma^\mu(1 - \gamma^5)u\frac{-ig_W}{2\sqrt{2}}$) currents.

This gives an inclusive (e, e') electron-nucleon scattering cross section that depends on only two structure func-

tions:

$$\frac{d^2\sigma^e}{dxdQ^2} = \frac{4\pi\alpha^2}{Q^4}\left[\frac{1-y}{x}F_2^e(x,Q^2) + y^2 F_1^e(x,Q^2)\right].\ (2)$$

Here F_1^e and F_2^e are the standard electromagnetic vector structure functions, $Q^2 = \mathbf{q}^2 - \omega^2$ is the squared momentum transfer and $\mathbf{q}$ and ω are the three-momentum and energy transfers, $x = Q^2/(2m\omega)$ is the Bjorken scaling variable, m is the nucleon mass, $y = \omega/E_e$ is the electron fractional energy loss, and α is the fine structure constant. This formula is valid for $Q^2 \gg m^2$ where the electron-nucleon cross section is simplest. Cross sections at lower Q^2 have more complicated factors multiplying each of the two structure functions.

The corresponding inclusive charged current (CC) $(\nu, l^\pm)$ neutrino-nucleon cross section (where $l^\pm$ is the outgoing charged lepton) has a similar form with the addition of third, axial, structure function:

$$\frac{d^2\sigma^\nu}{dxdQ^2} = \frac{G_F^2}{2\pi}\left[\frac{1-y}{x}F_2^\nu(x,Q^2) + y^2 F_1^\nu(x,Q^2)\right.$$
$$\left. -y(1-y/2)F_3^\nu(x,Q^2)\right].\ (3)$$

Here F_1^ν and F_2^ν are the neutrino-nucleus vector structure functions, F_3^ν is the axial structure function, and G_F is the Fermi constant. The parity-conserving structure functions, F_1^ν and F_2^ν, both include a vector-vector term identical to F_1^e and F_2^e, and an additional axial-axial term. See Refs. [1–3] for more detail.

These simple equations are very similar for lepton-nucleus scattering. In the limit of electron-nucleon elastic scattering ($x = 1$), the two structure functions reduce to the Dirac and Pauli form factors (which are linear combinations of the electric and magnetic form factors, $G_E(Q^2)$ and $G_M(Q^2)$). Neutrino-nucleon elastic scattering has an additional axial form factor. In the simplest case where a lepton scatters quasielastically from a nucleon in the nucleus and the nucleon does not reinteract as it leaves the nucleus, then the lepton-nucleus cross section is the integral over all initial state nucleons:

$$\frac{d\sigma}{dEd\Omega} = \int_{\mathbf{p_i}}\int_{E_b} d^3\mathbf{p_i}dE_b K S(\mathbf{p_i},E_b)\frac{d\sigma^{free}}{d\Omega}$$
$$\delta^3(\mathbf{q}-\mathbf{p_f}-\mathbf{p_r})\delta(\omega - E_b - T_f - T_r)\ (4)$$
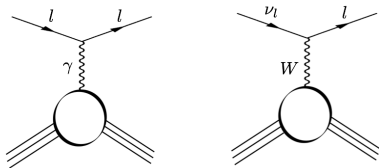
FIG. 1. (left) electron-nucleus inclusive scattering via one-photon exchange and (right) charged current neutrino-nucleus inclusive scattering via W exchange with a final state charged lepton.
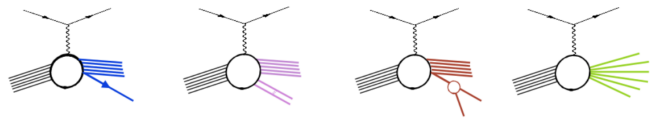
FIG. 2. Reaction mechanisms for lepton-nucleus scattering (a) quasielastic scattering (QE) where one nucleon is knocked out of the nucleus, (b) 2p2h where two nucleons are knocked out of the nucleus, (c) RES resonance production where a nucleon is excited to a resonance which decays to a nucleon plus meson(s), and (d) DIS where the lepton interacts with a quark in the nucleus.

where $\mathbf{p_i}$ and $\mathbf{p_f}$ are the initial and final momenta of the struck nucleon (in the absence of reinteraction, $\mathbf{p_f} = \mathbf{q} + \mathbf{p_i}$), $\mathbf{p_r} = -\mathbf{p_i}$ is the momentum of the recoil $A-1$ nucleus, E_b is the nucleon binding energy, $S(\mathbf{p_i}, E_b)$ is the probability of finding a nucleon in the nucleus with momentum $\mathbf{p_i}$ and binding energy E_b, T_f and T_r are the kinetic energies of the final state nucleon and $A-1$ system, $d\sigma^{free}/d\Omega$ is the lepton-bound nucleon elastic cross section, and K is a known kinematic factor.

This simple form is complicated for electrons and neutrinos by nucleon reinteraction which changes the overlap integral between the initial and final states (and thus the cross section), and changes the momentum and angle of the outgoing nucleon.

Thus, to calculate even the simplest type of lepton-nucleus interaction, we need to know the momentum and binding energy distribution of all nucleons in the nucleus, how the outgoing nucleon wave function is distorted by the nucleon-nucleus potential, and how the outgoing nucleon kinematics is changed by final state interactions.

In addition, the lepton can knock out two nucleons simultaneously, either by interacting with a nucleon belonging to a short range correlated (SRC) pair [4] or by interacting with a meson being exchanged between two nucleons. And, of course, these two interactions add coherently. The lepton can interact with a nucleon, exciting it to a resonance, which then deexcites resulting in emission of a nucleon plus mesons or of two nucleons. The lepton can also scatter inelastically from a quark in a nucleon. All of these different reaction mechanisms are very similar for electrons and for neutrinos. The outgoing hadrons in all of these interactions will interact identically with the residual nucleus, whether they are knocked out by an electron or by a neutrino.

This correspondence provides a valuable opportunity for rigorous tests of event generators: any generator model set which fails to accurately describe eA (vector) scattering data cannot be used with confidence to simulate νA (vector + axial-vector) interactions.

To demonstrate what can be learned by confronting a neutrino event generator with electron scattering data, we have created e-GENIE: a new electron-scattering version of the widely-used GENIE [5] event generator.

Whenever possible e-GENIE uses the same code and the same sets of physics models as the standard neutrino version.

Here we focus specifically on testing our current knowledge of $\sigma_i(E)$ by benchmarking e-GENIE against existing inclusive electron scattering data for different target nuclei at several incident beam energies and scattered electron angles. We find that the new SuSAv2 models describe the inclusive data better than the older ones, but resonance production reactions are still not well described, especially at larger momentum transfer.

Modeling

The most common lepton-nucleus interaction mechanisms include (Fig. 2): (a) quasielastic (QE) scattering from individual moving nucleons in the nucleus; (b) two-nucleon knockout, due to interactions with a meson being exchanged between two nucleons or to interactions with an SRC pair (refered to meson exchange current, MEC or two-particle two-hole excitations, $2p2h$); (c) interactions which leave the struck nucleon in an excited state (resonance production or RES); and (d) non-resonant interactions with a quark within the nucleon (DIS).

For fixed incident beam energy and scattered electron angle, the dominant process changes from QE at low energy transfer ($\omega \approx Q^2/2m$) through MEC to RES and to DIS at high energy transfer. Therefore, examining the agreement of e-GENIE with data as a function of energy transfer can provide valuable insight into the specific shortcomings of the e-GENIE models and their implementations.

The GENIE simulation framework offers several models of the nuclear ground state, several models for each of the eA or νA scattering mechanisms (each with various tunable model parameters), and several models for hadronic final state interactions (FSI), i.e., intranuclear rescattering of the outgoing hadrons [5, 6]. In this section, we describe the different models relevant for this work and the electron-specific effects that we accounted for during e-GENIE development.

Since our goal is to use electron scattering data to validate neutrino interaction modeling in GENIE, we chose to unify the GENIE code for electron and neutrino scattering modes wherever possible. The neutrino interacts with a nucleus via the weak interaction and massive W or Z exchange, whereas the electron interacts mostly electromagnetically via massless photon exchange, see Fig. 1. Both interactions probe the same nuclear ground state and many of the nuclear reaction effects are similar or identical. We thus constructed e-GENIE by setting the axial part of the interaction to zero and using cross sections that effectively differ by a factor of $\frac{8\pi^2\alpha^2}{G_F^2 Q^4}$ (see Eqs. 2 and 3).

When generating events for a beam of leptons with a continuously-distributed energy spectrum, GENIE samples an initial projectile energy E for each event using a probability density function of the form

$$P(E) \propto \Phi(E) \sum_i \sigma_i(E) \tag{5}$$

where Φ is the incident flux and the sum runs over the total cross sections σ_i for each available interaction mode (QE, MEC, RES, etc.). A specific mode j is then sampled with probability

$$P_j = \frac{\sigma_j(E)}{\sum_i \sigma_i(E)} . \tag{6}$$

GENIE does not include interference between the amplitudes of different reaction modes, i.e., the total cross section is obtained by adding the individual cross sections $\sigma_i(E)$ incoherently.

Many of the models reported in this work (except for SuSAv2) use the GENIE implementation of the local Fermi gas (LFG) model to describe the nuclear ground state. In a regular Fermi gas model, nucleons occupy all momentum states up to the global Fermi momentum k_F with equal probability. In the LFG model, the Fermi momentum at a given radial position depends on the local nuclear density (obtained from measurements of nuclear charge densities). To account for this radial dependence, GENIE selects an initial momentum for the struck nucleon by first sampling an interaction location r inside the nucleus according to the nuclear density. The nucleon momentum is then drawn from a Fermi distribution using the local Fermi momentum $k_F(r)$.

We consider two distinct sets of GENIE models for QE and MEC: those used in the G18_10a_02_11a configuration of GENIE v3.0.6 (referred to here as G2018) and chosen to describe data including mainly bubble chamber CCQE, CC1π, CC2π, CC inclusive and normalised topological cross-section data [7], and those used in the new SuSAv2 model set [8] approved for inclusion in the near-future GENIE v3.2 release as the GTEST19_10b_00_000 configuration and referred to here as SuSAv2. In both model sets, RES is modeled using the Berger-Sehgal model [9] and DIS reactions are modeled using Bodek and Yang[10]. These interactions are described in more detail below.

Quasi Elastic (QE)

In QE interactions, a lepton scatters on a single nucleon, removing it from the spectator $A-1$ nucleus unless final-state interactions lead to reabsorption.

The electron QE interaction in the G2018 configuration of GENIE uses the Rosenbluth cross section with the vector structure function parametrization of Ref. [11]. We corrected the implementation of this model for e-GENIE and modified the cross section as described

above. This electron QE cross section differs in important ways (notably, the Rosenbluth treatment lacks medium polarization corrections) from the Valencia CCQE model [12] used in the G2018 configuration for neutrinos.

A new QE model in GENIE, based on the SuSAv2 approach [8, 13, 14], uses superscaling to write the inclusive cross section in terms of a universal function (i.e., independent of momentum transfer and nucleus). For EM scattering, the scaling function may be expressed in the form

$$f(\psi') = k_F \frac{\frac{d^2\sigma}{d\Omega_e d\nu}}{\sigma_{Mott}(v_L G_L^{ee'} + V_T G_T^{ee'})}, \qquad (7)$$

where ψ' is a dimensionless scaling variable, k_F is the nuclear Fermi momentum, the denominator is the single-nucleon elastic cross section, v_L and v_T are known functions of kinematic variables, and $G_L^{ee'}(q,\omega)$ and $G_T^{ee'}(q,\omega)$ are the longitudinal and transverse nucleon structure functions (linearly related to F_1^e and F_2^e) [15]. For e-GENIE, we extended the original implementation for neutrinos [8] to the electron case using a consistent physics treatment.

The original SuSAv2 QE cross section calculations used a Relativistic Mean Field (RMF) model of the nuclear ground state [16, 17]. This approach includes the effects of the real part of the nucleon-nucleus potential on the outgoing nucleons which creates a "distorted" nucleon momentum distribution.

Although GENIE lacks the option to use an RMF nuclear model directly, we achieve approximate consistency with the RMF-based results by using a two-step strategy for QE event generation. First, an energy and scattering angle for the outgoing lepton are sampled according to the inclusive double-differential cross section. This cross section is computed by interpolating precomputed values of the nuclear responses $G_L^{ee'}(q,\omega)$ and $G_L^{ee'}(q,\omega)$ which are tabulated on a two-dimensional grid in (q,ω) space. The responses were obtained using the original RMF-based SuSAv2 calculation.

Second, the nucleon kinematics are determined by choosing its initial momentum from an LFG distribution. The default nucleon binding energy used in GENIE for the LFG model is replaced for SuSAv2 with an effective value tuned to most closely duplicate the RMF distribution. The outgoing nucleon kinematics are not needed for the comparisons to inclusive (e, e') data shown in this work.

Meson Exchange Current (MEC)

MEC describes an interaction that results in the ejection of two nucleons from the nucleus (often referred to as $2p2h$). It typically proceeds via lepton interaction with a pion being exchanged between two nucleons or by interaction with a nucleon in an SRC pair. GENIE has several models for MEC.

The G2018 configuration of e-GENIE uses the empirical Dytman model [18], that is useable for both eA and νA scattering. It assumes that the MEC peak for inclusive scattering has a Gaussian distribution in W and is located between the QE and first RES peaks. The amplitude of the MEC peak was tuned to electron scattering data. This model was developed in the context of empirically fitting GENIE to MiniBooNE inclusive neutrino scattering data.

For charged-current neutrino interactions, GENIE G2018 uses the very different Valencia $2p2h$ model [12, 19] instead of the empirical Dytman model, which is still used for neutral-current interactions.

Another MEC model, available for both eA and νA scattering, is the SuSAv2 MEC model [13, 20, 21]. The evaluation of the $2p2h$ MEC contributions is performed within an exact RFG-based microscopic calculation that englobes the $2p2h$ states excited by the action of meson-exchange currents within a fully relativistic framework [14, 22–24], and considers the weak vector and axial components for neutrino-nucleus interactions in both longitudinal and transverse channels as well as a complete analysis for electromagnetic reactions. As in the case for the SuSAv2 QE model, we extend the original GENIE implementation of SuSAv2 MEC for neutrinos [8] to the electron case for e-GENIE.

Resonance (RES) and Deep Inelastic Scattering (DIS)

Resonance production in GENIE is simulated using the Berger-Sehgal model [9], in which the lepton interacts with a single moving nucleon and excites it to one of 16 resonances. The cross sections are calculated based on the Feynman-Kislinger-Ravndal (FKR) model [25], without any interferences between them.

The GENIE treatment of deep inelastic scattering used in this work is based on that of Bodek and Yang [10]. Hadronization is modeled using an approach which transitions gradually between the AGKY model [26] and the PYTHIA 6 model [27]. At low values of the hadronic invariant mass W, the Bodek-Yang differential cross section is scaled by tunable parameters that depend on the multiplicity of hadrons in the final-state [6].

These parameters (together with a few others, such as the axial masses for CCQE and CCRES) were recently retuned by the GENIE collaboration to measurements of charged-current ν_μ and $\bar{\nu}_\mu$ scattering on deuterium [7]. The new tuning is included in the G2018 configuration but not in SuSAv2. The modeling of RES and DIS is otherwise identical.
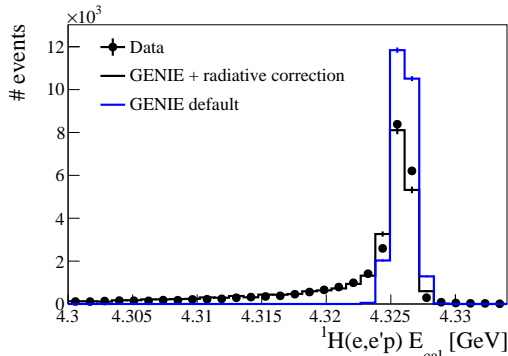
FIG. 3. Number of events vs $E_{cal} = E_{e'} + T_p$ the scattered electron energy plus proton kinetic energy for 4.32 GeV H$(e, e'p)$. Black points are data [31] , red histogram shows the unradiated GENIE prediction and blue histogram shows the GENIE prediction with electron radiation. The GENIE calculations have been scaled to have the same integral as the data.

Final State Interactions (FSIs)

The IntraNuclear Cascade (INC) model for FSI and hadronization is done in GENIE by the IN-TRANUKE [28, 29] package including two options. The first, hA, an empirical data-driven method, uses the cross-section of pions and nucleons with nuclei as a function of energy up to 1.2 GeV and the CEM03 [30] calculation normalised to low energy data for higher energies. The second, hN, is a full INC calculation of pions, kaons, photons, and nucleon interactions with nuclei up to 1.2 GeV.

The e-GENIE G2018 configuration uses the hA FSI model, while SuSAv2 uses hN. However, the choice of FSI model has no effect on the inclusive cross sections considered in the present work.

Radiative Corrections

When electrons scatter from nuclei, there are several radiative effects that change the cross section. The incoming and outgoing electrons can each radiate a real photon, which changes the kinematics of the interaction or the detected particles, and there can be vertex or propagator corrections that change the cross section. When comparing electron scattering data to models, either the data or the model needs to be corrected for radiative effects. Published electron scattering cross sections are typically corrected for radiative effects, but this correction is complicated and somewhat model-dependent.

We implemented a framework for electron radiative corrections in GENIE for the first time to allow comparisons to non-radiatively corrected data. The framework
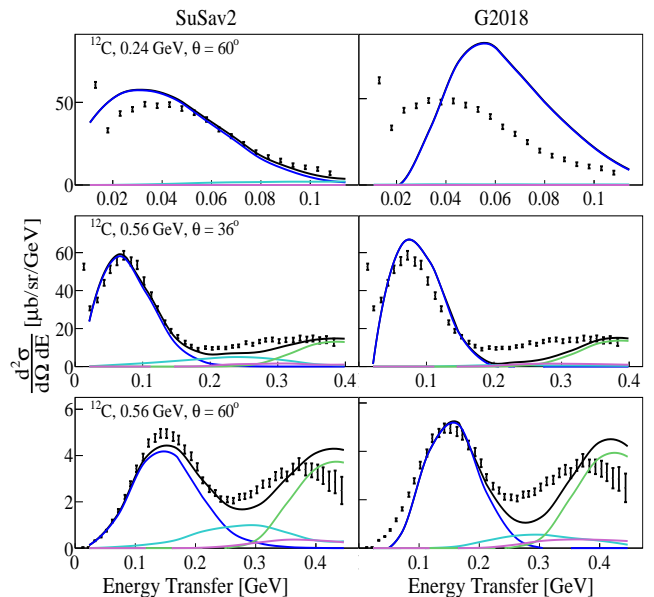
FIG. 4. Comparison of inclusive C(e, e') scattering cross sections for data and for GENIE. (left) data vs SuSAv2 and (right) data vs G2018. (top) $E_0 = 0.24$ GeV, $\theta_e = 60°$ and $Q^2_{QE} \approx 0.05$ GeV^2 [33], (middle) $E_0 = 0.56$ GeV, $\theta_e = 36°$ and $Q^2_{QE} \approx 0.11$ GeV^2 [33], and (bottom) $E_0 = 0.56$ GeV, $\theta_e = 60°$ and $Q^2_{QE} \approx 0.24$ GeV^2 [33]. Black points show the data, solid black lines show the total GENIE prediction, colored lines show the contribution of the different reaction mechanisms: (blue) QE, (magenta) MEC, (red) RES and (green) DIS.

allows electron radiation, which can change the kinematics of the event by changing either the incident or scattered electron energy (through radiation of a real photon). We modeled external radiation in the same way as the Jefferson Lab SIMC event generator [32]. Future versions of e-GENIE will incorporate cross section changes due to vertex and propagator corrections.

We validated the radiative correction procedure by comparing a simulated sample to electron scattering from protons at Jefferson Lab. Figure 3 shows the data compared to the GENIE simulation with and without radiative corrections. The radiatively corrected calculation is clearly much closer to the data. The radiative tail of the distribution is only significant for about 5 MeV below the peak.

This correction is used for comparisons with non-radiatively-corrected data. It was not used to compare with the radiatively-corrected inclusive data shown below.

e-GENIE comparisons to inclusive electron scattering data

To test e-GENIE, we compare inclusive electron scattering data to theoretical predictions made using two different program configurations which differ in their choice of
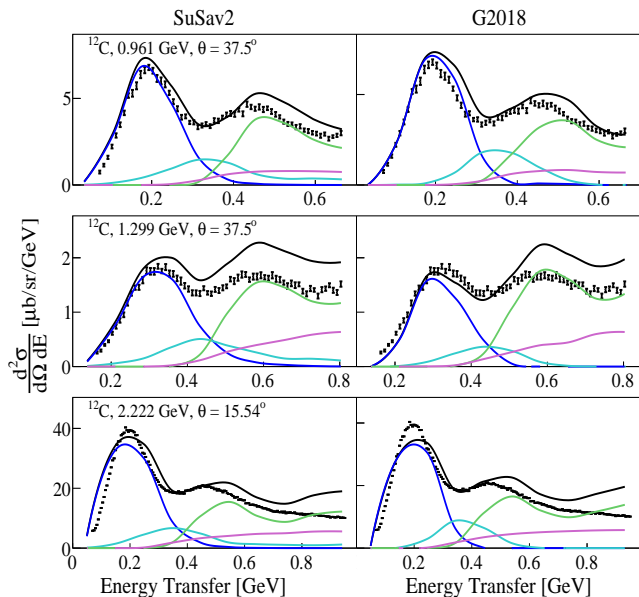
FIG. 5. Comparison of inclusive $C(e, e')$ scattering cross sections for data and for GENIE. (left) data vs SuSAv2 and (right) data vs G2018. (top) $E_0 = 0.96$ GeV, $\theta_e = 37.5°$ and $Q^2_{QE} \approx 0.32$ GeV^2 [34], (middle) $E_0 = 1.30$ GeV, $\theta_e = 37.5°$ and $Q^2_{QE} \approx 0.54$ GeV^2 [34], and (bottom) $E_0 = 2.22$ GeV, $\theta_e = 15.5°$ and $Q^2_{QE} \approx 0.33$ GeV^2 [35]. Black points show the data, solid black lines show the total GENIE prediction, colored lines show the contribution of the different reaction mechanisms: (blue) QE, (magenta) MEC, (red) RES and (green) DIS.

FIG. 6. Comparison of inclusive $C(e, e')$ scattering cross sections for data and for GENIE. (left) data vs SuSAv2 and (right) data vs G2018. (top) $E_0 = 1.501$ GeV, $\theta_e = 37.5°$ and $Q^2_{QE} \approx 0.92$ GeV^2 [34], (middle) $E_0 = 3.595$ GeV, $\theta_e = 16°$ and $Q^2_{QE} \approx 1.04$ GeV^2 [36], and (bottom) $E_0 = 3.595$ GeV, $\theta_e = 20°$ and $Q^2_{QE} \approx 1.3$ GeV^2 [36]. Black points show the data, solid black lines show the total GENIE prediction, colored lines show the contribution of the different reaction mechanisms: (blue) QE, (magenta) MEC, (red) RES and (green) DIS.

QE and MEC models: G2018 (which adopts the Rosenbluth model for QE and the empirical Dytman model for MEC) and SuSAv2 (which adopts SuSAv2 for both QE and MEC).

Figs. 4, 5 and 6 show the inclusive $C(e, e')$ cross sections for a wide range of beam energies and scattering angles compared to the G2018 and SuSAv2 models. The QE peak is the one at lowest energy transfer ($\nu \approx Q^2/2m$) in each plot. The next peak at about 300 MeV larger energy transfer corresponds to $\Delta(1232)$ excitation and the "dip region" is between the two peaks. SuSAv2 clearly describes the QE and dip regions much better than G2018, especially at the three lowest momentum transfers (see Fig. 4). G2018 has particular difficulty describing the data for $E_0 = 0.24$ GeV and $\theta_e = 60°$, where $Q^2 = 0.05$ GeV^2 at the quasielastic peak. G2018 also predicts too small a width for the quasielastic peak and too small a 2p2h/MEC contribution for $E_0 = 0.56$ GeV and $\theta_e = 60°$. At higher incident energies, SuSAv2 describes the data better than G2018, although it overpredicts the dip region cross section at $E_0 = 1.299$ GeV and $\theta_e = 37.5°$. Both model sets significantly disagree with the data in the resonance region (where they use the same RES and DIS models).

Fig. 7 shows the inclusive $Ar(e, e')$ cross sections for

$E_0 = 2.222$ GeV and $\theta_e = 15.54°$ [37] compared to the G2018 and SuSAv2 models. Both models reproduce the data moderately well in the QE, dip and Δ-peak regions, but there is again significant disagreement at larger energy transfers.

Fig. 8 shows the inclusive $Fe(e, e')$ cross sections for several beam energies and scattering angles compared to the G2018 and SuSAv2 models. The SuSAv2 model describes the QE region better for all three data sets. The SuSAv2 model describes the dip region significantly better for the two lower energies, but overpredicts the cross section there at the highest energy. The disagreement near the Δ peak is a bit smaller for the Fe data than the corresponding C data.

Summary

We implemented an electron version of GENIE, the popular neutrino-nucleus event generator. This new version of GENIE is designed to use the same cross section models and the same event generation machinery as the neutrino version, in order to rigorously test the vector current part of the lepton-nucleus interaction. We also added partial radiative corrections for electron scattering.

We compared two different GENIE model sets to in-
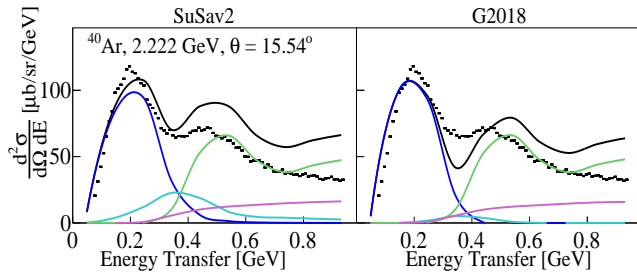
FIG. 7. Comparison of inclusive $Ar(e, e')$ scattering cross sections for data and for GENIE at $E_0 = 2.22$ GeV, $\theta_e = 15.5°$ and $Q^2_{QE} \approx 0.33$ GeV^2 [37]. (left) data vs SuSAv2 and (right) data vs G2018. Black points show the data, solid black lines show the total GENIE prediction, colored lines show the contribution of the different reaction mechanisms: (blue) QE, (magenta) MEC, (red) RES and (green) DIS.
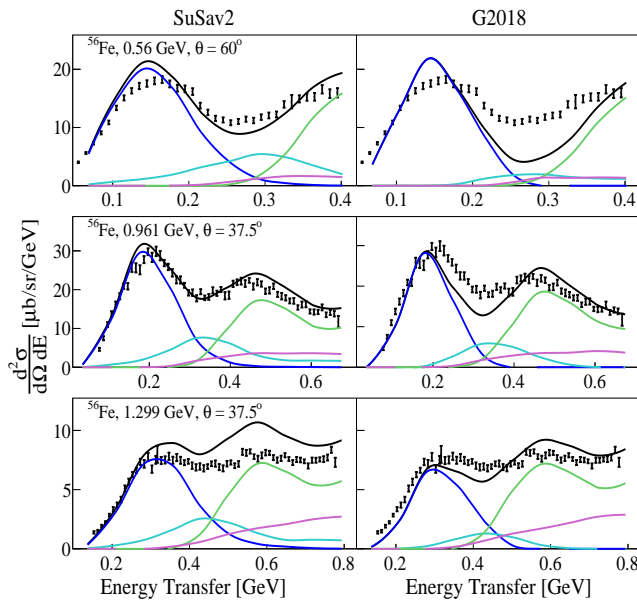
FIG. 8. Comparison of inclusive $Fe(e, e')$ scattering cross sections for data and for GENIE. (left) data vs SuSAv2 and (right) data vs G2018. (a) $Fe(e, e')$, $E_0 = 0.96$ GeV, $\theta_e = 37.5°$ and $Q^2_{QE} \approx 0.32$ GeV^2 [34], (b) $Fe(e, e')$, $E_0 = 1.30$ GeV, $\theta_e = 37.5°$ and $Q^2_{QE} \approx 0.54$ GeV^2 [34]. Black points show the data, solid black lines show the total GENIE prediction, colored lines show the contribution of the different reaction mechanisms: (blue) QE, (magenta) MEC, (red) RES and (green) DIS.

clusive electron-scattering data for a wide range of targets, beam energies and scattering angles. The G2018 and SuSAv2 model sets differ in their description of QE and MEC scattering. Both models describe the data at least moderately well in the QE and MEC regions. The SuSAv2 model set describes the QE and MEC regions in most of the data sets better than G2018. However, at the highest momentum transfers, e-GENIE dramatically overpredicts the data, indicating significant prob-

lems with the momentum-transfer dependence of the RES and DIS models used.

By developing an electron version of GENIE that uses the same reaction mechanism models as the standard neutrino version, we have prepared the machinery to test the vector current part of the lepton-nucleus interaction against more extensive, and more exclusive, electron scattering data sets. This should provide enough information to allow us to improve the vector current interactions in neutrino event generators, which should improve the precision of future neutrino oscillation experiments.

* Contact Author adishka@mit.edu
[1] L. Alvarez-Ruso *et al.*, Prog. Part. Nucl. Phys. **100**, 1 (2018), arXiv:1706.03621 [hep-ph].
[2] T. Katori and M. Martini, J. Phys. G **45**, 013001 (2018), arXiv:1611.07770 [hep-ph].
[3] J. Amaro, M. Barbaro, J. Caballero, R. Gonzlez-Jimnez, G. Megias, and I. Ruiz Simo, (2019), arXiv:1912.10612 [nucl-th].
[4] O. Hen, G. A. Miller, E. Piasetzky, and L. B. Weinstein, Rev. Mod. Phys. **89**, 045002 (2017).
[5] C. Andreopoulos, A. Bell, D. Bhattacharya, F. Cavanna, J. Dobson, S. Dytman, H. Gallagher, P. Guzowski, R. Hatcher, P. Kehayias, A. Meregaglia, D. Naples, G. Pearce, A. Rubbia, M. Whalley, and T. Yang, Nucl. Inst. and Meth. A **614**, 87 (2010), 0905.2517.
[6] C. Andreopoulos, C. Barry, S. Dytman, H. Gallagher, T. Golan, R. Hatcher, G. Perdue, and J. Yarba, (2015), arXiv:1510.05494 [hep-ph].
[7] J. Tena-Vidal, "Tuning the pion production with GENIE version 3," https://indico.cern.ch/event/703880/contributions/3157410/, talk delivered at the 12th International Workshop on Neutrino-Nucleus Interactions in the Few-GeV Region (NuInt 18).
[8] S. Dolan, G. D. Megias, and S. Bolognesi, Phys. Rev. D **101**, 033003 (2020).
[9] C. Berger and L. Sehgal, Phys. Rev. D **76**, 113004 (2007), arXiv:0709.4378 [hep-ph].
[10] A. Bodek and U. K. Yang, Journal of Physics G: Nuclear and Particle Physics **29**, 1899 (2003), hep-ex/0210024.
[11] R. Bradford, A. Bodek, H. S. Budd, and J. Arrington, Nucl. Phys. B Proc. Suppl. **159**, 127 (2006), arXiv:hep-ex/0602017.
[12] J. Nieves, I. R. Simo, and M. J. V. Vacas, Phys. Rev. C **83**, 045501 (2011), 1102.2777.
[13] G. D. Megias, J. E. Amaro, M. B. Barbaro, J. A. Caballero, and T. W. Donnelly, Phys. Rev. D **94**, 013012 (2016).
[14] G. Megias, J. Amaro, M. Barbaro, J. Caballero, T. Donnelly, and I. Ruiz Simo, Phys. Rev. D **94**, 093004 (2016), arXiv:1607.08565 [nucl-th].
[15] J. Caballero, Phys. Rev. C **74**, 015502 (2006), arXiv:nucl-th/0604020.
[16] R. Gonzlez-Jimnez, A. Nikolakopoulos, N. Jachowicz, and J. Udas, Phys. Rev. C **100**, 045501 (2019), arXiv:1904.10696 [nucl-th].
[17] R. Gonzlez-Jimnez, M. Barbaro, J. Caballero, T. Don-

nelly, N. Jachowicz, G. Megias, K. Niewczas, A. Nikolakopoulos, and J. Udas, Phys. Rev. C **101**, 015503 (2020), arXiv:1909.07497 [nucl-th].

[18] T. Katori, AIP Conf. Proc. **1663**, 030001 (2015), arXiv:1304.6014 [nucl-th].

[19] J. Schwehr, D. Cherdack, and R. Gran, (2017), 1601.02038.

[20] G. Megias *et al.*, Phys. Rev. D **91**, 073004 (2015), arXiv:1412.1822 [nucl-th].

[21] J. E. Amaro, M. B. Barbaro, J. A. Caballero, A. De Pace, T. W. Donnelly, G. D. Megias, and I. Ruiz Simo, Phys. Rev. C **95**, 065502 (2017).

[22] A. De Pace, M. Nardi, W. Alberico, T. Donnelly, and A. Molinari, Nucl. Phys. A **741**, 249 (2004), arXiv:nucl-th/0403023.

[23] I. Ruiz Simo, J. Amaro, M. Barbaro, A. De Pace, J. Caballero, and T. Donnelly, J. Phys. G **44**, 065105 (2017), arXiv:1604.08423 [nucl-th].

[24] I. Ruiz Simo, C. Albertus, J. Amaro, M. Barbaro, J. Caballero, and T. Donnelly, Phys. Rev. D **90**, 033012 (2014), arXiv:1405.4280 [nucl-th].

[25] R. P. Feynman, M. Kislinger, and F. Ravndal, Phys. Rev. D **3**, 2706 (1971).

[26] T. Yang, C. Andreopoulos, H. Gallagher, K. Hofmann, and P. Kehayias, The European Physical Journal C **63**, 1 (2009), 0904.4043.

[27] T. Sjöstrand, S. Mrenna, and P. Skands, Journal of High Energy Physics **2006**, 026 (2006), hep-ph/0603175.

[28] S. Dytman and A. Meyer, AIP Conference Proceedings **1405**, 213 (2011).

[29] R. Merenyi, W. A. Mann, T. Kafka, W. Leeson, B. Saitta, J. Schneps, M. Derrick, and B. Musgrave, Phys. Rev. D **45**, 743 (1992).

[30] S. G. Mashnik, A. J. Sierk, K. K. Gudima, and M. I. Baznat, J. Phys. Conf. Ser. **41**, 340 (2006).

[31] R. Cruz-Torres *et al.* (Jefferson Lab Hall A Tritium), Phys. Lett. B **797**, 134890 (2019), arXiv:1902.06358 [nucl-ex].

[32] "Simc monte carlo," https://hallcweb.jlab.org/wiki/ index.php/SIMC_Monte_Carlo (2020).

[33] P. Barreau *et al.*, Nucl. Phys. A **402**, 515 (1983).

[34] R. M. Sealock, K. L. Giovanetti, S. T. Thornton, Z. E. Meziani, O. A. Rondon-Aramayo, S. Auffret, J.-P. Chen, D. G. Christian, D. B. Day, J. S. McCarthy, R. C. Minehart, L. C. Dennis, K. W. Kemper, B. A. Mecking, and J. Morgenstern, Phys. Rev. Lett. **62**, 1350 (1989).

[35] H. Dai *et al.* (Jefferson Lab Hall A), Phys. Rev. C **98**, 014617 (2018), arXiv:1803.01910 [nucl-ex].

[36] D. Day *et al.*, Phys. Rev. C **48**, 1849 (1993).

[37] H. Dai *et al.* (The Jefferson Lab Hall A Collaboration), Phys. Rev. C **99**, 054608 (2019).